

# Photoproduction of $\eta'$ -mesons from the Proton

A. Sibirtsev<sup>1,2</sup>, Ch. Elster<sup>2,1</sup>, S. Krewald<sup>1</sup>, and J. Speth<sup>1</sup>

<sup>1</sup>*Institut für Kernphysik, Forschungszentrum Jülich, D-52425 Jülich, Germany*

<sup>2</sup>*Institute of Nuclear and Particle Physics, Ohio University, Athens, OH 45701*

(September 20, 2018)

## Abstract

The presently available data for the reaction  $\gamma p \rightarrow \eta' p$  are analyzed in terms of a model in which the dominant production mechanism is the exchange of the vector mesons  $\omega$  and  $\rho$ . To describe the data at photon energies close to the production threshold we introduce a resonance contribution due to the well established  $S_{11}(1535)$  resonance. Finally we study the contributions due to nucleon exchange to the  $\eta'$  photoproduction and find, that those contributions can be seen at large angles in the differential cross section.

arXiv:nucl-th/0303044v1 18 Mar 2003

Typeset using REVTeX

## I. INTRODUCTION

The investigation of the production of  $\eta'$  mesons in hadron and photon induced reactions provides direct access to low energy QCD dynamics. The intrinsic properties of the  $\eta'$  meson are dominated by the gluonic degrees of freedom and continue to attract theoretical and experimental interest since the first observation of  $\eta'$  mesons [1,2] in the reaction  $K^-p \rightarrow \Lambda\eta'$  at LBL and BNL in 1964.

The mass of the  $\eta'$  meson is substantially larger than the ones of the other mesons from the pseudoscalar meson nonet. Therefore, the  $\eta'$  meson could not be considered as pure pseudoscalar Goldstone boson with a mass generated by spontaneous chiral symmetry breaking. However, the strong chiral  $U_A(1)$  anomaly in QCD allows the  $\eta'$  meson to gain additional mass by different mechanisms [3–9]. The large mass of the  $\eta'$  meson can be viewed as being generated essentially by non-perturbative gluon dynamics and the  $U_A(1)$  axial anomaly.

Furthermore, an anomalous gluon not only generates a large  $\eta'$  meson mass, but also affects the dynamics of the  $\eta'$ -nucleon interaction. The flavor singlet Goldberger-Treiman relation correlates [10–15] the  $\eta'$ -nucleon coupling constant,  $g_{\eta'NN}$ , and the flavor singlet axial charge of the nucleon,  $g_A^0$ , and in the chiral limit [16,17] one has

$$g_A^0 = \sqrt{\frac{3}{2}} \frac{F_0}{m_N} (g_{\eta'NN} - g_{GNN}). \quad (1)$$

Here  $m_N$  is the nucleon mass,  $F_0=0.1$  GeV renormalizes the flavor singlet decay constant [11,18], and  $g_{GNN}$  is the gluon-nucleon coupling [11]. Moreover,  $g_A^0$  can be decomposed in terms of the quark and gluon spin components of the proton [19,20].

Unexpectedly, a very small value of  $g_A^0=0.2 \div 0.35$  was extracted from EMC measurements [21] of the polarized proton structure function. In a naive parton interpretation, i.e. neglecting the gluonic degrees of freedom by taking  $g_{GNN}=0$ , the EMC result indicates that the quark contribution to the proton spin,  $\Delta\Sigma = \sqrt{3/2} g_{\eta'NN} F_0/m_N$ , is compatible with zero. This interpretation has supported speculations either about the validity of experimental results and data analysis or the applicability of perturbative QCD. Alternatively, the spin crisis can be resolved by substituting a large positive value,  $g_{GNN} \simeq 2.45$ , and substantial cancellation between the quark and gluon spin components. It was suggested [14,22], that instead of the gluon component the contribution from the  $\eta'$  meson is canceled by the higher mass states, which are either radial excitations of the  $\eta'$  meson or glueball states.

At present, the two component interpretation of the axial charge is generally accepted. However, both  $g_{\eta'NN}$  and  $g_{GNN}$  coupling constants are not known individually. The origin of the proton spin and its decomposition in terms of quark and gluon degrees of freedom still remain controversial. However, it is believed that the coupling constant  $g_{\eta'NN}$  defines up to large extent the total spin of the nucleon carried by its constituents.

It is important to note that the coupling constant  $g_{\eta'NN}$  may experimentally be accessible in nuclear reactions involving the coupling between the  $\eta'$  meson and the nucleon.

The reaction  $pp \rightarrow pp\eta'$  was intensively studied at COSY [23–26] and SATURNE [27–29]. Theoretical calculations [30–33] allow a description of the data entirely by the meson exchange currents. It was found that the contribution of the nucleon current to the  $\eta'$  meson

production in proton-proton collisions is small. Thus the reaction  $pp \rightarrow pp\eta'$  is not well suited for the direct evaluation of the coupling constant  $g_{\eta'NN}$ . Additional measurements of differential cross sections and more detailed theoretical studies are necessary to determine under what conditions the nucleon exchange current may dominate the meson exchange or may be at least partially isolated.

Experimental information [34] about the reactions  $\pi^- p \rightarrow \eta' n$  and  $\pi^+ n \rightarrow \eta' p$  is insensitive to the contribution from the nucleon exchange, although in principle these reactions would be well suited for the determination of the coupling constant  $g_{\eta'NN}$ . Here the situation may be substantially improved with new and precise data for  $\eta'$  meson production at large angles, where the nucleon current dominates.

The reaction  $\gamma p \rightarrow \eta' p$  was studied by a number of collaborations, namely ABBHHM [35], AHHM [36] and SAPHIR [37,38]. While ABBHHM and AHHM measured only the total cross section for the photoproduction of the  $\eta'$  meson at photon energies  $1.67 \leq E_\gamma \leq 5$  GeV, the SAPHIR collaboration at ELSA studied the angular spectra of the  $\eta'$  mesons produced at photon energies  $0.9 \leq E_\gamma \leq 2.6$  GeV. In addition, the photoproduction of  $\eta'$  mesons from the nucleon is presently experimentally investigated by the CLAS Collaboration at TJNAF [39] and by the Crystal Barrel Collaboration at ELSA.

Currently experimental and theoretical [40–45] studies of the reaction  $\gamma p \rightarrow \eta' p$  are motivated by the possibility to investigate excited baryons coupled to the  $\eta'$  meson. Assuming that the resonance production is the dominant contribution, an isobar analysis [37] of the SAPHIR data shows that the  $\eta'$ -photoproduction at photon energies  $0.9 \leq E_\gamma \leq 2.6$  GeV can be described by the coherent excitation of two resonances,  $S_{11}(1897)$  and  $P_{11}(1986)$ . However, the presently available data [35–38] for the  $\eta'$ -photoproduction are quite limited. Thus, an evaluation of resonance properties from these data should be considered with caution. It is also clear that the contribution from the meson exchange current to the reaction  $\gamma p \rightarrow \eta' p$  can not be completely neglected, as was shown in the analysis of the reaction  $pp \rightarrow pp\eta'$ .

Here we investigate up to what extent present data for the reaction  $\gamma p \rightarrow \eta' p$  can be described by the exchange of vector mesons in the  $t$  channel and the nucleon exchange in the  $s$  and  $u$  channels. We do not consider contributions from baryonic resonances with masses above the production threshold. If possible resonances will significantly contribute to the production mechanism, then a discrepancy between our calculation and data should indicate this.

In addition, we aim to investigate the conditions under which the nucleon exchange current can be well controlled, and whether the reaction  $\gamma p \rightarrow \eta' p$  may be used to better determine the coupling constant  $g_{\eta'NN}$ .

## II. VECTOR MESON EXCHANGE AS PRODUCTION MECHANISM

One of the well established results in particle physics is that for very high energies, i.e.  $E_\gamma > 5$  GeV, Regge trajectories provide the dominant processes for peripheral reactions. At energies well below 5 GeV, but still clearly above the resonance region the photoproduction of mesons can be described the  $t$  channel meson exchanges. In our case the photoproduction of the  $\eta'$  meson is dominated by the exchanges of the  $\rho$  and the  $\omega$  meson. The relevant Feynman diagrams are shown in Fig. 1. The four momenta of the initial nucleon and photon

and the final nucleon and  $\eta'$  meson are denoted as  $p_i$ ,  $k$ ,  $p_f$  and  $q$ , respectively.

We use the Mandelstam invariants to define the reaction kinematics and invariant reaction amplitudes, namely

$$\begin{aligned} s &= (p_i + k)^2 = (p_f + q)^2 = m_N^2 + 2m_N E_\gamma \\ t &= (p_i - p_f)^2 = (k - q)^2 \\ u &= (k - p_f)^2 = (p_i - q)^2 = 2m_N^2 + m_{\eta'}^2 - t - s. \end{aligned} \quad (2)$$

The relation between the four momentum transfer squared and the scattering polar angle  $\theta$  is given as

$$t = m_{\eta'}^2 - 2q^0 k^0 + 2|\mathbf{q}||\mathbf{k}| \cos \theta. \quad (3)$$

Thus,  $\eta'$  meson photoproduction at backward angles,  $\cos \theta = -1$ , corresponds to the maximal four momentum transfer squared,  $-t$ , and increases with increasing the photon energy  $E_\gamma$ . Moreover the maximal  $-t$  corresponds to the minimal value of  $|u|$ . At the production threshold for  $\eta'$  mesons the squared invariant collision energy is given by  $s = (m_N + m_{\eta'})^2$ , and the invariant  $t$  takes the form

$$t = -\frac{m_N m_{\eta'}^2}{m_N + m_{\eta'}} = -0.45 \text{ GeV}^2. \quad (4)$$

From Eq. (4) it is obvious, that already at the reaction threshold the  $\eta'$  meson photoproduction probes large  $|t|$ . Thus, the  $\rho$  and  $\omega$  meson exchanges should be very sensitive [46] to the choice of the form factors at the nonlocal interaction vertices. The shaded area in Fig. 2 shows the range of the four momenta transfer squared  $t$  accessible in the reaction  $\gamma N \rightarrow \eta' N$  at a given photon energy  $E_\gamma$ , or at a given squared invariant collision energy  $s$ . The figure shows clearly that for the energies available at ELSA and TJNAF, namely  $E_\gamma < 2.5$  GeV, the photoproduction of  $\eta'$ - mesons probes large  $|t|$  up to  $\simeq -3$  GeV<sup>2</sup>.

Furthermore, it is important to notice that uncertainties in the  $t$ -channel contributions due to unknown coupling constants and form factors can be eliminated through data collected at energies slightly beyond the resonance region. Here the  $t$ -channel contributions dominate at the low four momentum transfer squared. We also note that at high energies,  $E_\gamma > 5$  GeV, the elementary particle exchange should be generalized to the correct expression for the exchange of a Regge trajectory with physical coupling constants comprising the residue [47–49]. Thus, the availability of precision data at photon energies  $2 < E_\gamma < 5$  GeV is very crucial for the theoretical analysis of  $t$ -channel exchanges.

The effective Lagrangian densities used for the evaluation of the vector meson ( $V$ ) exchange amplitudes are given as [50–56]

$$\mathcal{L}_{VNN} = g_V \bar{N} \gamma_\mu N V^\mu + \frac{g_T}{2m_N} \bar{N} \sigma_{\mu\nu} N V^{\mu\nu} \quad (5)$$

$$\mathcal{L}_{V\eta'\gamma} = \frac{eg_V \eta' \gamma}{m_{\eta'}} \varepsilon_{\mu\nu\alpha\beta} F^{\mu\nu} V^{\alpha\beta} \eta'. \quad (6)$$

Here  $m_{\eta'}$  stands for the mass of the  $\eta'$  meson,  $m_N$  for the mass of the nucleon. The vector meson field tensor is given by  $V_{\mu\nu} = \partial_\nu V_\mu - \partial_\mu V_\nu$ , and  $F^{\mu\nu} = \partial_\nu A_\mu - \partial_\mu A_\nu$  with  $A^\mu$  being the photon field.

The vector ( $g_V$ ) and tensor ( $g_T$ ) coupling constants at the  $\omega NN$  and  $\rho NN$  vertices are adopted from the Bonn potential model [57]. As in the NN potential model, we dress the vertices with monopole form factors,

$$F_{VNN}(t) = \frac{\Lambda_{VNN}^2 - m_V^2}{\Lambda_{VNN}^2 - t}, \quad (7)$$

with  $m_V$  being the mass of the vector meson. We adopt the cut-off parameter  $\Lambda_{VNN}=1.5$  GeV from the Bonn model, as well as the coupling constants  $g_{\rho NN}=3.9$  and  $g_{\omega NN}=10.6$ . The ratio of the tensor to vector coupling is 6.1 for the  $\rho$  meson and zero for the  $\omega$  meson.

The couplings for the  $\rho\eta'\gamma$  and  $\omega\eta'\gamma$  vertices can be evaluated from the partial decay widths of the reactions  $\eta'\rightarrow\gamma\rho$  and  $\eta'\rightarrow\omega\rho$ . The two quantities are related by

$$\Gamma_{\eta'\rightarrow\gamma V} = \frac{e^2 g_{V\eta'\gamma}^2 (m_{\eta'}^2 - m_V^2)^3}{32\pi m_{\eta'}^5}, \quad (8)$$

where  $e^2=4\pi\alpha$ , with  $\alpha$  being the electromagnetic coupling. With  $\Gamma_{\rho\rightarrow\gamma\eta'}=60\pm 5$  keV and  $\Gamma_{\omega\rightarrow\gamma\eta'}=6.1\pm 0.8$  keV we obtain  $g_{\rho\eta'\gamma}=1.36$ , and  $g_{\omega\eta'\gamma}=0.4$ .

The form factors at the  $\rho\eta'\gamma$  and  $\omega\eta'\gamma$  vertices are not fixed by the model. As shown in Fig. 2(a), the  $\eta'$ - meson photoproduction probes a large region of  $|t|$ . Thus we expect that our calculations may be very sensitive to the choice of the unknown form factor at the  $V\eta'\gamma$  vertex. Moreover, because of an anomalous gluon component, the structure function of the  $\eta'$  meson is different from the one for mesons which are built up from quark-antiquark configurations. In a meson exchange model the intrinsic structure of the  $\eta'$  meson enters effectively through the form factors at the  $\rho\eta'\gamma$  and  $\omega\eta'\gamma$  vertices, which do not necessarily have to be of the standard monopole or dipole type [40–44]. In principle, the form factor at large  $|t|$  is given by the meson structure function at short distances and in case of  $\eta'$  meson might be defined through its gluon component.

For our calculations we adopt an exponential form factor

$$\tilde{F}_{V\eta'\gamma}(t) = \exp(\tilde{\Lambda}_{V\eta'\gamma} t), \quad (9)$$

with  $\tilde{\Lambda}_{V\eta'\gamma}=1.2$  GeV<sup>-2</sup> being our best choice value obtained by adjusting to the  $\eta'$  meson photoproduction data. Its behavior as function of the four momentum squared,  $-t$ , is shown by the solid line in Fig. 2(b). As comparison we show in the same figure as dashed line the monopole form factor of Eq. (7) with the standard [57] cut-off parameter  $\Lambda_{VNN}=1$  GeV. For this comparison, the exponential form factor is renormalized to  $F_{VNN}(t)=1$  at  $t=m_\rho^2$ , where  $m_\rho$  being the  $\rho$  meson mass. While the exponential and monopole form factors are almost identical for small  $|t|$ , i.e.  $|t|<0.8$  GeV<sup>2</sup>, the difference at large  $-t$  is quite obvious.

Finally, the four Lorentz and gauge invariant amplitudes [58] for the reaction  $\gamma p\rightarrow\eta'p$  due to the vector meson exchanges are given as

$$\begin{aligned} A_1 &= \frac{eg_{V\eta'\gamma}}{m_{\eta'}} \frac{g_T}{2m_N} \frac{t}{t - m_V^2} \\ A_1 + tA_2 &= 0 \\ A_3 &= 0 \\ A_4 &= -\frac{eg_{V\eta'\gamma}g_V}{m_{\eta'}} \frac{1}{t - m_V^2}. \end{aligned} \quad (10)$$

It is understood that each amplitude contains in addition the product of the form factors at the  $VNN$  and  $V\eta'\gamma$  vertices.

The differential cross section for the photoproduction of  $\eta'$  mesons due to the vector meson exchange is obtained from

$$\frac{d\sigma}{dt} = \frac{F_{VNN}^2(t)F_{V\eta'\gamma}^2(t)}{16\pi(s - m_N^2)^2} \sum_{i,j=1}^4 Q_{i,j} \sum_{\rho,\omega} A_i \sum_{\rho,\omega} A_j^*, \quad (11)$$

where  $Q_{ij}$  are the well known [59,60] hermitian matrix elements given in terms of Mandelstam invariants.

In Figs. 3 and 4 we display the differential cross sections for the reaction  $\gamma p \rightarrow \eta' p$  measured by the SAPHIR collaboration at ELSA [37,38]. We choose to plot the cross section  $d\sigma/dt$  instead of the angular spectra [37,38], since in this case the slope with respect to  $t$  explicitly indicates the strength of the form factor. Thus, the  $t$  scale provides an appropriate representation of the data collected at large four momentum transfer squared.

The solid lines in Figs. 3 and 4 represents our results obtained with an exponential form factor  $\tilde{F}_{V\eta'\gamma}(t)$  at the  $\omega\eta'\gamma$  and  $\rho\eta'\gamma$  vertices with  $\tilde{\Lambda}_{V\eta'\gamma}=1.2 \text{ GeV}^{-2}$ , and they reproduce for photon energies  $E_\gamma \geq 1.9 \text{ GeV}$  quite reasonably.

As a motivation of the form factor at the  $\rho\eta'\gamma$  and  $\omega\eta'\gamma$  vertices we analyze the experimental differential cross sections in a parameterized form as

$$\frac{d\sigma}{dt} = A \exp(bt). \quad (12)$$

The slope  $b$  and the constant  $A$  are shown in ig. 5 as function of the invariant collision energy  $\sqrt{s}$ . It should be noted that  $A$  here does not represent the magnitude of the differential cross section at  $t=0$ , as can be well understood from Fig.2, but an extrapolated value.

Within experimental uncertainties the slope  $b$  does not depend on the energy and can be well fitted by a constant value  $b=1.8 \pm 0.2 \text{ GeV}^{-2}$ , as is shown by the solid line in Fig.5(b). The  $t$  dependence at low four momentum transfer squared beyond the resonance region is dominated by the vector exchange contribution. Therefore, the slope  $b=1.8 \text{ GeV}^{-2}$  at  $\sqrt{s} > 2 \text{ GeV}$  can be linked to the form factor at the  $\rho\eta'\gamma$  and  $\omega\eta'\gamma$  vertices.

Possible contribution from other  $\eta'$  meson photoproduction mechanisms might change the slope  $b$  at lower energies. If the  $\eta'$  meson couples to additional resonances, the exponential slope of  $t$  dependence may increase or decrease in the resonance region, depending whether an interference between the resonant and vector meson exchange contributions is destructive or constructive. The size of the change of the slope with the photon energy will depend on the strength of the resonance coupling to  $\eta'$  meson. However, as we found the uncertainties of the data are still too large to clarify this feature.

Finally, since both, the slope of the  $t$  dependence of  $\eta'$  meson photoproduction cross section and the constant  $A$  do not depend on the energy at  $\sqrt{s} > 2.0 \text{ GeV}$ , we adjust the cut off parameter  $\tilde{\Lambda}_{V\eta'\gamma}=1.2 \text{ GeV}^{-2}$  at these energies through [46] the logarithmic derivative of the differential cross section. The solid line in Fig. 5 shows the local slope at  $t=-0.6 \text{ GeV}^2$  evaluated as

$$b(t, \sqrt{s}) = \frac{d}{dt} \ln \left[ \frac{d\sigma}{dt} \right], \quad (13)$$

with the differential cross section for the reaction  $\gamma p \rightarrow \eta' p$  given by Eq. (11).

We also want to compare our calculation based on an exponential form factor  $\tilde{\Lambda}_{V\eta'\gamma}$  to a calculation, where we employ a standard monopole form factor at the  $\omega\eta'\gamma$  and  $\rho\eta'\gamma$  vertices. The dashed lines in Figs. 3 and 4 show such a calculation with a cut-off parameter  $\Lambda_{V\eta'\gamma}=1.5$  GeV at the  $\omega\eta'\gamma$  and  $\rho\eta'\gamma$  vertices. This value is identical to the one at the  $\omega NN$  and  $\rho NN$  vertices. We see that a calculation with a monopole form factor at the electromagnetic vertices can not reproduce the  $t$  dependence of the  $\eta'$  meson photoproduction data especially at photon energies above 1.7 GeV. It should not be surprising, that form factors as the vertices with the vector mesons coupling to the nucleon are different from the ones where the vector mesons couple to the photon, since the internal structure of those vertices is different.

The comparison between the SAPHIR data [37,38] and our calculations based on vector meson exchange as sole production mechanism leads to the following conclusions. First, a comparison of the calculations to the data for small photon energies,  $E_\gamma \leq 1.6$  GeV, shows some room for a possible contributions from  $s$  wave resonances. However, we do not see much room for the contribution from the  $p$  wave resonance, which must introduce an additional  $t$  dependence. Second, the differential cross section at  $E_\gamma=2.1$  GeV seems to indicate some enhancement at maximal  $-t$  or small  $|u|$ , which can not be explained by considering vector meson exchange alone. Indeed, this enhancement may point to the importance of considering the nucleon exchange as part of the production mechanism.

### III. CONTRIBUTIONS FROM BARYON RESONANCES

The possibility of studying excited baryons which couple to the  $\eta'$  meson in the reaction  $\gamma p \rightarrow \eta' p$  initiated considerable theoretical activity [40–45], in which contributions from a number of resonances were introduced. For example, the approach of Refs. [40,41], based on effective Lagrangians, considers nine baryonic resonances in different partial waves. These are two  $S_{11}$  resonances as  $N^*(2030)$  and  $N^*(2090)$ , three  $D_{13}$  resonances as  $N^*(2055)$ ,  $N^*(2080)$  and  $N^*(2095)$ , two  $D_{15}$  resonances,  $N^*(2080)$  and  $N^*(2200)$  and one  $F_{17}$  resonance,  $N^*(1990)$ . Contributions from only the  $S_{11}(2090)$ ,  $P_{11}(2100)$  and  $P_{13}(1900)$  resonances are discussed in the Regge model calculation of Ref. [45]. In contrast, the quark model calculation of Ref. [42] considers only a  $S_{11}(1535)$  resonance.

Because of the large uncertainties in the experimental results and the very limited number of experimental points [37,38] presently available for the reaction  $\gamma p \rightarrow \eta' p$ , we prefer to introduce as few resonances into our calculation as possible. It is also clear, that large uncertainties in the selection of the parameters of potential resonances, i.e. mass and width, the coupling to the  $\eta'$  meson as well as our lack of knowledge about relevant form factors at the resonance vertices might provide quite a large freedom in describing the present data by isobar contributions. Having this in mind, and considering our results from Figs. 3 and 4, we see that we mostly underpredict the present data close to the reaction threshold. Overall, we find that the data can be reasonably well described by a single production mechanism, namely the exchange of vector mesons. It is also clear that this exchange of vector mesons can be reggeized [45], providing it is applicable at the very high energies. Thus, concluding from Fig. 5 we only have room for additional contributions at photon energies  $E_\gamma < 1.7$  GeV, or at

invariant collision energies below 2 GeV. Furthermore, since the slope  $b$  of the  $t$  dependence does not change at  $E_\gamma < 1.7$  GeV, we also do not see room for the contribution from any  $p$  wave (or higher partial wave) resonances.

A closer look at Fig.5(a) reveals, that this possible additional contribution dominates already at the  $\eta'$  meson photoproduction threshold,  $\sqrt{s} \simeq 1896$  MeV, decreases with increasing photon energy and almost vanishes for  $\sqrt{s} \simeq 2010$  MeV. Since the differential cross section,  $d\sigma/dt$ , given in Eq.(11) does not contain a final phase space factor, the constants  $A$  can be considered as being proportional to the squared averaged reaction matrix element, which has a maximum value at threshold and saturates with increasing the photon energy. Thus we guess that energies with  $1896 \leq \sqrt{s} \leq 2010$  MeV (see Fig.2(a)) are influenced by the tale of a resonance which has a pole at or below the  $\eta'$  meson photoproduction threshold.

Since there are little constraints on resonances coupled to the  $\eta'$  meson, different choices of  $s$  wave resonances having masses below 1896 MeV are in principle possible. In general, the interaction Lagrangians for a  $N(\frac{1}{2}^\pm)$  nucleon resonances are given as [50–54]

$$\begin{aligned}\mathcal{L}_{\eta'NR} &= -ig_{\eta'NR} \bar{R} \Gamma N \eta' + \text{h.c.}, \\ \mathcal{L}_{\gamma NR} &= e \bar{R} \frac{\kappa_R^S + \kappa_R^V \tau_3}{2(m_N + m_R)} \tilde{\Gamma} \sigma_{\mu\nu} N F^{\mu\nu} + \text{h.c.},\end{aligned}\quad (14)$$

where  $m_R$  denotes the resonance mass,  $R$  the field operator of the resonance, and  $\kappa_R^S$  and  $\kappa_R^V$  are the isoscalar and isovector transition magnetic couplings. The vertex functions for nucleon resonances  $R$  with negative parity are  $\Gamma=1$  and  $\tilde{\Gamma}=\gamma_5$ , while resonances with positive parity have  $\Gamma=\gamma_5$  and  $\tilde{\Gamma}=1$ .

Furthermore, for a proton target  $\kappa_R^p = \kappa_R^S + \kappa_R^V$  and the relation between the magnetic coupling and the helicity amplitude  $A_{1/2}^p$  is given by [54,61,62]

$$|A_{1/2}^p|^2 = \left( \frac{e\kappa_R^p}{m_N + m_R} \right)^2 \frac{m_R^2 - m_N^2}{2m_N}. \quad (15)$$

For a neutron target one has  $\kappa_R^n = \kappa_R^S - \kappa_R^V$ , and the helicity amplitudes  $R \rightarrow p\gamma$  and  $R \rightarrow n\gamma$  are given by the Particle Data Group [63]. We take  $\kappa_R = 2.3$ . The couplings of the  $\eta'$  meson to baryon resonances,  $g_{\eta'NR}$ , are generally unknown and can only be adjusted to data. In our calculation a value  $g_{\eta'RN} = 3.4$  is adopted.

Finally, the invariant amplitudes for  $s$ - and  $u$ -channel nucleon resonance contributions can be written as

$$\begin{aligned}A_1 &= \pm \frac{eg_{\eta'NR}\kappa_R(m_N \pm m_R)}{m_N + m_R} \left[ \frac{1}{s-m_R^2} + \frac{1}{u-m_R^2} \right], \\ A_2 &= 0 \\ A_3 &= \pm \frac{eg_{\eta'NR}\kappa_R}{m_N + m_R} \left[ \frac{1}{s-m_R^2} - \frac{1}{u-m_R^2} \right], \\ A_3 &= \pm \frac{eg_{\eta'NR}\kappa_R}{m_N + m_R} \left[ \frac{1}{s-m_R^2} + \frac{1}{u-m_R^2} \right],\end{aligned}\quad (16)$$

where the plus sign is assigned to the negative parity excited state, while the minus sign corresponds to positive parity excited state. The coupling  $\kappa_R$  stands for the magnetic coupling for a proton or a neutron target.



Furthermore, we include form factors at the interaction vertices, because an excited, intermediate baryon resonance is off shell. In our calculations we employ an overall formfactor with the general form [64]

$$F(u, s) = F(u) + F(s) - F(u)F(s). \quad (17)$$

The individual formfactors in the  $u$  and  $s$  channels are given by

$$F(r) = \frac{\Lambda_R^4}{\Lambda_R^4 - (r - m_R^2)^2}. \quad (18)$$

Here  $r=s$  or  $u$ , and the cut off parameter  $\Lambda_R$  is adjusted to the data. In our calculations we use  $\Lambda_R=1$  GeV, and take the same values for both, the  $u$  and the  $s$  channels.

To study the influence of s-wave resonances on the behavior of the differential cross section close to the production threshold, we prefer to select only the well known  $S_{11}(1535)$  resonance and investigate, whether its contribution is sufficient to account for the difference between our calculation based on vector meson exchange alone and the data for photon energies  $E_\gamma < 1.7$  GeV.

Our calculations including the contribution of the resonance  $S_{11}(1535)$  as well as the vector meson exchange is shown as solid line in Fig. 6 in comparison to the data for photon energies  $1.5 \leq E_\gamma \leq 2.1$  GeV. The dashed line represents the calculation with the vector meson exchange alone. The resonant contribution dominates around the  $\eta'$  meson photoproduction threshold and vanishes with increasing the photon energy.

Concluding this section we want to emphasize that our calculations do not prove that resonant contributions to the  $\eta'$  meson photoproduction are not necessarily only those from the  $S_{11}(1535)$  resonance. Large uncertainties in selection of the coupling constants  $g_{\eta'NR}$  to resonances as well as in cutoff parameters  $\Lambda_R$  allow sufficient freedom to consider more resonant contributions. However, in this work, we did not prefer to include any other resonance than  $S_{11}(1535)$ .

#### IV. CONTRIBUTION OF THE NUCLEON EXCHANGE

Since the mass of the  $\eta'$  meson is close to the nucleon mass, the range of the squared four momentum  $u$  available in the reaction  $\gamma p \rightarrow \eta' p$  is almost the same as the range of the variable  $t$  as is indicated in Fig. 2. As  $-u$  approaches its minimal value, the contribution from the nucleon exchange increases due to the  $u$  dependence of the squared nucleon propagator,  $(u - m_N^2)^{-2}$ .

To map out the  $u$  dependence of the differential cross section, it is worthwhile to perform the measurements at sufficiently large photon energies, which provide access to a wide range of  $u$ . In addition, at large energies the separation between the  $t$  and the  $u$  channel becomes more pronounced. At the same time, the  $s$  channel contribution from the nucleon exchange is small because of the  $s$  dependence of the squared nucleon propagator,  $(s - m_N^2)^{-2}$ .

Obviously, baryon resonances may also contribute at small  $|u|$ . However, they contribute at the same time to the  $s$  channel and fill the gap between small  $-t$  and small  $-u$ . Though it may not be possible to evaluate resonance properties unambiguously from the data, the

overall resonant contribution can be fitted, as we illustrated in the previous section. Thus the resonant background to the  $u$  channel nucleon exchange contribution can be well estimated and subtracted.

In general, the contribution from the nucleon exchange current can be measured at small  $u$  or at backward angles in meson photoproduction reaction. Obviously, the size of the contribution will depend on the strength of the coupling of the  $\eta'$  meson to the nucleon. In fact, such an increase of the differential cross section at small  $u$  was detected in the photoproduction of  $\pi$  and  $\omega$  mesons [65,66]. Thus, it may also be observed in the photoproduction of  $\eta'$  mesons.

The effective Lagrangians for the  $\gamma NN$  and  $\eta' NN$  interaction can be written as [67]

$$\begin{aligned}\mathcal{L}_{\gamma NN} &= -e\bar{N}\left(\gamma_\mu\frac{1+\tau_3}{2}A^\mu - \frac{\kappa^S + \kappa^V\tau_3}{4m_N}\sigma_{\mu\nu}F^{\mu\nu}\right)N \\ \mathcal{L}_{\eta' NN} &= -ig_{\eta' NN}\bar{N}\gamma_5 N\eta'.\end{aligned}\tag{19}$$

Here  $\kappa^S$  and  $\kappa^V$  are the isoscalar and isovector anomalous magnetic moments of the nucleon,  $\kappa_p = \kappa^S + \kappa^V = 1.79$  and while  $\kappa_n = \kappa^S - \kappa^V = -1.91$  stand for the proton and neutron, respectively.

The four invariant amplitudes for the  $\eta'$  meson photoproduction due to the nucleon exchange current in  $s$  and  $u$  channels are given as

$$\begin{aligned}A_1 &= e_N e g_{\eta' NN} \left[ \frac{1}{s - m_N^2} + \frac{1}{u - m_N^2} \right], \\ A_2 &= \frac{2e_N e g_{\eta' NN}}{(s - m_N^2)(u - m_N^2)}, \\ A_3 &= -\frac{e g_{\eta' NN} \kappa_N}{2m_N} \left[ \frac{1}{s - m_N^2} - \frac{1}{u - m_N^2} \right], \\ A_4 &= -\frac{e g_{\eta' NN} \kappa_N}{2m_N} \left[ \frac{1}{s - m_N^2} + \frac{1}{u - m_N^2} \right],\end{aligned}\tag{20}$$

where  $e_N=0$  for a neutron and  $e_N=1$  for a proton target. In principle, we should consider formfactors at the interaction vertices, since the nucleons are off shell in the intermediate state. However, the introduction of a form factor violates gauge invariance. To prevent this, we use the form factor given by Eqs.(17,18) with a cutoff parameter  $\Lambda_N=800$  MeV.

As we discussed in the introduction, the coupling constant  $\eta' NN$  is unknown and we suggest the possibility to obtain information and constraints on it from the  $\eta'$  meson photoproduction data at small  $|u|$ . However, within accuracy of the present data shown in Fig. 7, it is quite speculative to discuss additional contributions and any enhancement of the differential cross section for the reaction  $\gamma p \rightarrow \eta' p$  at small  $|u|$ . Thus, for the present calculations of the nucleon exchange contribution we only estimate the size of the  $\eta' NN$  coupling constant.

Because of the  $SU(3)$  breaking the pseudoscalar octet mixes with the corresponding pseudoscalar singlet to produce the physical  $\eta$  and  $\eta'$  meson states. Taking the  $\eta$ - $\eta'$  mixing angle  $\theta \simeq -20^\circ$  and the ratio of the singlet to octet constants  $\simeq \sqrt{2}$  [68], the  $\eta NN$  and  $\eta' NN$  coupling constants can be related as

$$\frac{g_{\eta'NN}}{g_{\eta NN}} = \frac{\sin \theta + \sqrt{2} \cos \theta}{\cos \theta - \sqrt{2} \sin \theta}. \quad (21)$$

A theoretical analysis [53,54] of the  $\eta$  meson photoproduction data gives  $2.7 \leq g_{\eta NN} \leq 8.9$  and consequently  $1.9 \leq g_{\eta' NN} \leq 6.1$ . Estimates based on  $SU(6)$  [69] give  $g_{\eta' NN} = 6.5$ .

The  $\eta' NN$  coupling constant was also extracted from experimental observables. An old analysis [71] based on  $NN$  potentials gives  $g_{\eta NN} = 6.8$  and  $g_{\eta' NN} = 7.3$ , while nucleon-nucleon forward dispersion relations [70] yield  $g_{\eta NN}^2 + g_{\eta' NN}^2 \leq 12$ . Calculations of the decay  $\eta' \rightarrow \gamma\gamma$  with baryon triangle contributions [72] give  $g_{\eta' NN} = 6.3$ . Although, the  $\eta' NN$  constant extracted from different experiments is in a reasonable agreement with the  $SU(3)$  estimates, the exact value is still considered as being model dependent, since the gluonic component of the  $\eta'$  meson was neglected. For example, in  $NN$  scattering the gluon-nucleon interaction generates a contact term and may reduce the extracted value of the  $\eta' NN$  coupling constant.

Neglecting the gluon-nucleon coupling  $g_{GNN}$  in Eq.(1) one can estimate the  $\eta' NN$  coupling constant as  $g_{\eta' NN} \simeq 2.2$ . This value can be considered as quite small, as we discussed in the introduction. On the other hand, the OZI predictions [73,74] for the axial charge of the nucleon, neglecting the polarized strange quark and gluon contributions to the internal spin structure of the nucleon, gives  $g_A^0 \simeq 0.6$ . Attributing this value to the  $\eta' NN$  coupling constant one can estimate  $g_{\eta' NN} \simeq 4.6$ . The more careful analysis [15] based on the Goldberger-Treiman relation for the axial charge gives  $g_{\eta' NN} = 3.4$

For our calculations we adjust the coupling constant  $\eta' NN$  within the above listed boundaries to the data and use  $g_{\eta' NN} = 2.9$ . The solid lines in Fig. 7 shows our calculations for the  $\eta'$  photoproduction cross section based on the contribution from the vector meson exchange, the  $S_{11}(1535)$  resonance and the nucleon exchange current. As we can see, the quality of the presently available data, especially at large  $|t|$ , is such, that it is not useful to estimate any uncertainty of value of  $g_{\eta' NN}$ . However our calculations presented in Fig. 7 clearly illustrate that the differential cross section for  $\eta'$  meson photoproduction at small  $|u|$  or at large scattering angles can be used for a determination of the  $\eta' NN$  coupling constant.

## V. SUMMARY AND CONCLUSIONS

Our goal was to describe the reaction  $\gamma p \rightarrow \eta' p$  from threshold to photon energies  $E_\gamma = 2.4$  GeV. First we studied the contribution from vector meson exchange in the  $t$  channel to the  $\eta'$  meson photoproduction cross section. With this, the presently available data from the SAPHIR collaboration at ELSA [37,38] can be well reproduced for photon energies  $E_\gamma \geq 1.8$  GeV to 2.4 GeV.

The discrepancy between our calculation based on vector meson exchange alone and the data at small photon energies,  $1.5 \leq E_\gamma < 1.7$  GeV, may be attributed to contributions of resonances. An analysis of the data in terms of the energy dependence of the extrapolated forward differential cross section  $d\sigma/dt$  supports the assumption that this additional contribution results from a resonance with a mass below the  $\eta'$  meson production threshold. Thus we include the well established  $S_{11}(1535)$  nucleon resonance into our calculation. Finally we can describe the available data for  $1.5 \leq E_\gamma \leq 2.4$  GeV quite well. However we note, that with the presently available data we can not conclude that the  $S_{11}(1535)$  resonance is the only one that contributes to the reaction  $\gamma p \rightarrow \eta' p$ .

As last step we investigated the contribution from the nucleon exchange to the reaction  $\gamma p \rightarrow \eta' p$ . The aim is to see whether this contribution can be detected experimentally. Our calculations show that the nucleon exchange contribution dominates at small  $|u|$  for photon energies  $E_\gamma \geq 1.8$  GeV. Our speculation is that an experimental measurement under the above kinematical conditions can be used for a better evaluation of the contribution from the nucleon exchange, which in turn allows to obtain the  $\eta' NN$  coupling constant. Because of the large uncertainties of available estimates for the  $\eta' NN$  coupling constant and its importance for the clarification of proton spin crisis problem [8,10,12–14], a precise measurement of the  $\eta'$  meson photoproduction at large angles is crucial.

### ACKNOWLEDGMENTS

This work was performed in part under the auspices of the U. S. Department of Energy under contract No. DE-FG02-93ER40756 with the Ohio University. The authors appreciate very useful discussions and communications with M. Dugger, J. Ernst, E. Pasyuk and B.G. Ritchie. A.S would like to acknowledge the warm hospitality of the Department of Physics and Astronomy at Ohio University during his visit.

## REFERENCES

- [1] G.R. Kalbfleisch et al., Phys. Rev. Lett. **12**, 527 (1964).
- [2] M. Goldberg et al., Phys. Rev. Lett. **12**, 546 (1964).
- [3] S. Weinberg, Phys. Rev. D **11**, 3583 (1975).
- [4] A.D. Rejula, H. Georgi and S.L. Glashow, Phys. Rev. D **12**, 147 (1975).
- [5] G.'t Hooft, Phys. Rev. Lett. **37**, 8 (1976).
- [6] G.'t Hooft, Phys. Rev. D **14**, 3432 (1976).
- [7] E. Witten, Nucl. Phys. B **156**, 269 (1979).
- [8] G. Veneziano, Nucl. Phys. B **159**, 213 (1979).
- [9] G. Christos, Phys. Rept. **116**, 251 (1984).
- [10] G. Veneziano, Mod. Phys. Lett. A **4**, 1605 (1989).
- [11] G.M. Shore and G. Veneziano, Nucl. Phys. B **381**, 23 (1992).
- [12] T. Hatsuda, Nucl. Phys. B **329**, 376 (1990).
- [13] A.V. Efremov, J. Soffer and N.A. Törnqvist, Phys. Rev. D **44**, 1369 (1991).
- [14] K. Chao, J.R. Wen, H. Zheng, Phys. Rev. D **46**, 5078 (1992).
- [15] H.Y. Cheng, Chin.J.Phys.**34**, 738 (1996).
- [16] G.M. Shore and G. Veneziano, Phys. Lett. B **244**, 75 (1990).
- [17] S.D. Bass, S. Wetzel and W. Weise, Nucl. Phys. A **686**, 429 (2001).
- [18] S.D. Bass Phys. Lett. B **463**, 286 (1999)
- [19] G. Altarelli and G.G. Ross, Phys. Lett. B **212**, 391 (1988).
- [20] R.D. Carlitz, J.C. Collins and A.H. Mueller, Phys. Lett. B **214**, 229 (1988).
- [21] J. Ashman et al., Nucl. Phys. B **328**, 1 (1989).
- [22] X. Ji, Phys. Rev. Lett. **65**, 408 (1990).
- [23] P. Moskal et al., Phys. Rev. Lett. **80**, 3202 (1998)
- [24] P. Moskal et al., Phys. Lett. B **474**, 416 (2000).
- [25] A. Khoukaz et al., Nucl. Phys. A **663**, 565 (2000).
- [26] P. Moskal et al., Phys. Lett. B **482**, 356 (2000).
- [27] F. Hibou et al., Phys. Lett. B **438**, 41 (1998).
- [28] W. Kuhn et al., Nucl. Phys. A **663**, 569 (2000).
- [29] F. Balestra et al., Phys. Lett. B **491**, 29 (2000).
- [30] A. Sibirtsev and W. Cassing, Eur. Phys. J. A **2**, 333 (1998).
- [31] V. Bernard, N. Kaiser and U.-G. Meissner, Eur. Phys. J. A **4**, 259 (1999).
- [32] V. Baru, J. Haidenbauer, A. Kudryavtsev, P. Moskal and J. Speth, Eur. Phys. J. A **6**, 445 (1999).
- [33] K. Nakayama, H.F. Arellano, J.W. Durso, J. Speth, Phys. Rev. C **61**, 024001 (2000).
- [34] Landolt-Börnstein, New Series I/12, ed. H. Schopper, Springer-Verlag (1988).
- [35] ABBHMM Collaboration, Phys. Rev. **175**, 1669 (1968).
- [36] W. Struczinski et al., Nucl. Phys. B **108**, 45 (1976);
- [37] R. Plotzke et al., Phys. Lett. B **444**, 555 (1998).
- [38] J. Barth et al., Nucl. Phys. A **691**, 374 (2001).
- [39] M. Dugger, Ph.D. Thesis, ASU, 2001.
- [40] J.F. Zhang, N.C. Mukhopadhyay and M. Benmerrouche, Phys. Rev. C **52**, 1134 (1995).
- [41] J.F. Zhang, N.C. Mukhopadhyay and M. Benmerrouche, PiN Newslett. **10**, 81 (1995).
- [42] Z.P. Li, J. Phys. G **23**, 1127 (1997).

- [43] B. Borasoy, Eur. Phys. J. A **9**, 95 (2000).
- [44] B. Borasoy, E. Marco and S. Wetzela, Phys. Rev. C **66**, 055208 (2002).
- [45] W.T. Chiang, S.N. Yang, L. Tiator, M. Vanderhaeghen and D. Drechsel, nucl-th/0212106.
- [46] A. Sibirtsev, S. Krewald and A.W. Thomas, nucl-th/0301082.
- [47] A. Donnachie and P.V. Landshoff, Phys. Lett. B **348**, 213 (1995).
- [48] A. Donnachie and P.V. Landshoff, Phys. Lett. B **478**, 146 (2000).
- [49] A. Sibirtsev, K. Tsushima and S. Krewald, nucl-th/0301015
- [50] N. Levy, W. Majerotto and B.J. Read, Nucl. Phys. B **55**, 493 (1973)
- [51] M.G. Olsson and E.T. Osypowski, Nucl. Phys. B **87**, 399 (1975).
- [52] M.G. Olsson and E.T. Osypowski, Phys. Rev. D **17**, 174 (1978).
- [53] M. Benmerrouche and N.C. Mukhopadhyay, Phys. Rev. Lett. **67**, 1070 (1991).
- [54] M. Benmerrouche and N.C. Mukhopadhyay, Phys. Rev. D **51**, 3237 (1995).
- [55] K. Tsushima, A. Sibirtsev and A.W. Thomas, Phys. Lett. B **390**, 29 (1997).
- [56] K. Tsushima, A. Sibirtsev and A.W. Thomas, Phys. Rev. C **59**, 369 (1999).
- [57] R. Machleidt, K. Holinde and C. Elster, Phys. Rept. **149**,1 (1987).
- [58] G.F. Chew, M.L. Goldberger. F.E. Low and Y. Nambu, Phys. Rev. **106**, 1345 (1957).
- [59] E. Amaldi, S. Fubini and G. Furlan, Pion Electroproduction, Springer, Berlin (1979).
- [60] R. Williams, C.R. Ji and S.R. Cotanch, Phys. Rev. D **41**, 1449 (1990).
- [61] A.N. Mitra and M. Ross, Phys. Rev. **158**, 1630 (1967).
- [62] L.A. Copley, G. Karl and E. Obryk, Nucl. Phys. B **13**, 303 (1969).
- [63] Particle Data Group, Eur. Phys. J. C **15**, 1 (2000).
- [64] R.M. Davidson and R. Workman, Phys. Rev. C **63**, 025210 (2001).
- [65] R.L. Anderson et al. Phys. Rev. Lett. **23**, 721 (1969)
- [66] R.W. Clift et al. Phys. Lett. B **64**, 213 (1976).
- [67] F. Gross, J.W. Van Orden and K. Holinde, Phys. Rev. C **41**, 1909 (1990).
- [68] R. Koniuk and N. IZgur, Phys. Rev. D **21**, 1868 (1980).
- [69] N. Törnqvist and P. Zenczykowski, Phys. Rev. D **29**, 2139 (1984).
- [70] W. Grein and P. Kroll, Nucl. Phys. A **338**, 332 (1980).
- [71] O. Dumbrajs et al., Nucl. Phys. B **216**, 277 (1983).
- [72] B. Bagchi and A. Lahiri, J. Phys. G **16**, 239 (1990).
- [73] J. Ellis and R.L. Jaffe, Phys. Rev. D **9**, 1444 (1974).
- [74] J. Ellis and R.L. Jaffe, Phys. Rev. D **10**, 1669 (1974).

## FIGURES

FIG. 1. Diagrams contributing to the photoproduction of the  $\eta'$  meson from a nucleon: (a) denotes the vector meson exchange of  $\omega$  and  $\rho$ , (b) the u-channel contribution of the nucleon N (or resonance R) exchange, and (c) stands for the corresponding s-channel contribution.

FIG. 2. The shaded area in (a) shows the range of  $t$  and  $s$  accessible in reaction  $\gamma N \rightarrow \eta' N$  at the photon energy  $E_\gamma$  given on the upper axis. In (b) the behavior of the monopole (dashed) and exponential (solid line) form factors are shown as function of the four momentum transfer squared  $-t$ . The form factors are shown for  $\Lambda_V=1.0$  GeV and  $\tilde{\Lambda}_{V\eta'\gamma}=1.2$  GeV<sup>-2</sup> and normalised  $F_{V\eta'\gamma}(t)=1$  at  $t=m_\rho^2$ .

FIG. 3. The differential cross section for the reaction  $\gamma p \rightarrow \eta' p$  as a function of the four momentum transfer squared  $t$ . The squares represent the first SAPHIR results given in Ref. [37] with absolute normalization. The circles stand for new SAPHIR data reported in Ref. [38] in relative normalization, which we multiply by a factor of 2.9 at all given photon energies  $E_\gamma$ . The lines represent our calculations, for the solid line the exponential form factor  $\tilde{F}_{V\eta'\gamma}(t)$  of Eq. (9) at the vertices  $\gamma\rho\eta'$  and  $\gamma\omega\eta'$  is employed, for the dashed line the monopole form factor  $F_{V\eta'\gamma}(t)$  of Eq. (7) is used.

FIG. 4. Same as in Fig. 3 for different photon energies  $E_\gamma$ .

FIG. 5. The extrapolated forward  $\eta'$  meson photoproduction cross section (a) and the slope  $b$  of the  $t$  dependence (b) as a function of the invariant collision energy. The squares show the first SAPHIR results from Ref. [37] with absolute normalization, while the circles are new SAPHIR data reported in Ref. [38] in relative normalization and multiplied by a factor of 2.9. The arrows indicate the reaction threshold. The dashed line in (b) shows the fit by a constant value  $b=1.8\pm 0.2$  GeV<sup>-2</sup>, while the solid line uses the local slope at  $t=-0.6$  GeV<sup>2</sup> resulting from our calculations with Eq. (13).

FIG. 6. The differential cross section for the reaction  $\gamma p \rightarrow \eta' p$  as function of four momentum transfer squared  $t$ . The squares show the first SAPHIR results given in Ref. [37] with absolute normalization. The circles are new SAPHIR data reported in Ref. [38] in relative normalization, which we multiply by a factor of 2.9 at all given photon energies  $E_\gamma$ . The dashed line represents our calculation with the vector meson exchange alone as production mechanism (corresponding to the solid line in Figs. 3 and 5). The solid line includes in addition the contribution from the  $S_{11}(1535)$  resonance.

FIG. 7. The differential cross sections for the  $\eta'$  meson photoproduction as a function of four momentum transfer squared  $t$  at different photon energies  $E_\gamma$ . The squares show the first SAPHIR results given [37] with absolute normalization. The circles are new SAPHIR data reported [38] in relative normalization, which we multiply by a factor of 2.9 at all given photon energies  $E_\gamma$ . The solid line represents our calculation including vector meson exchange, the contribution from the  $S_{11}(1535)$  resonance as well as the contribution from the nucleon exchange. For the calculation shown as dashed line, the contribution from the nucleon exchange was omitted.



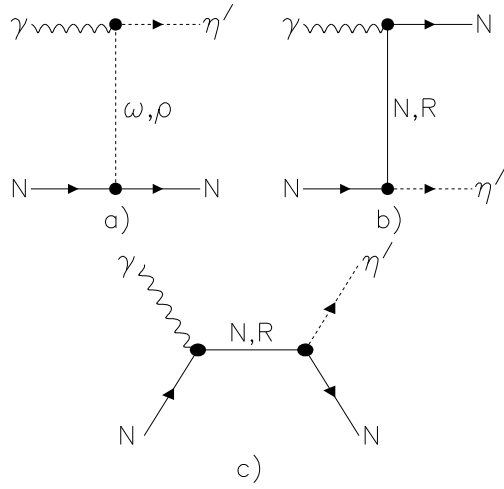


FIG. 1

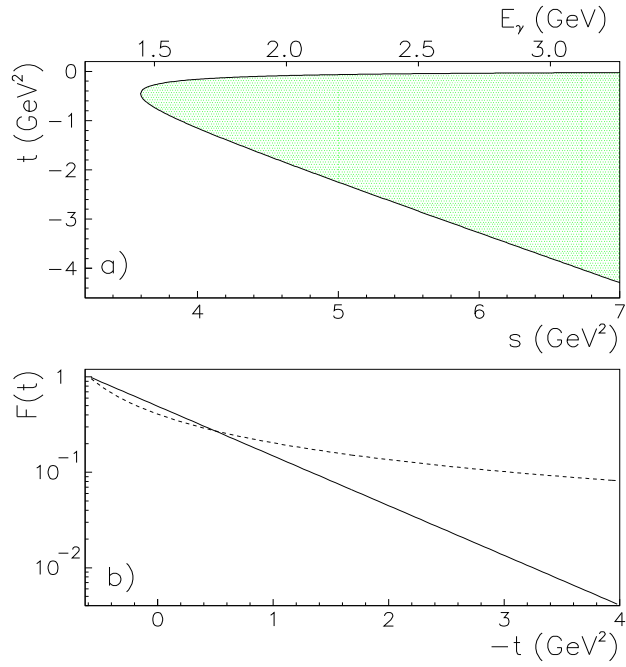


FIG. 2

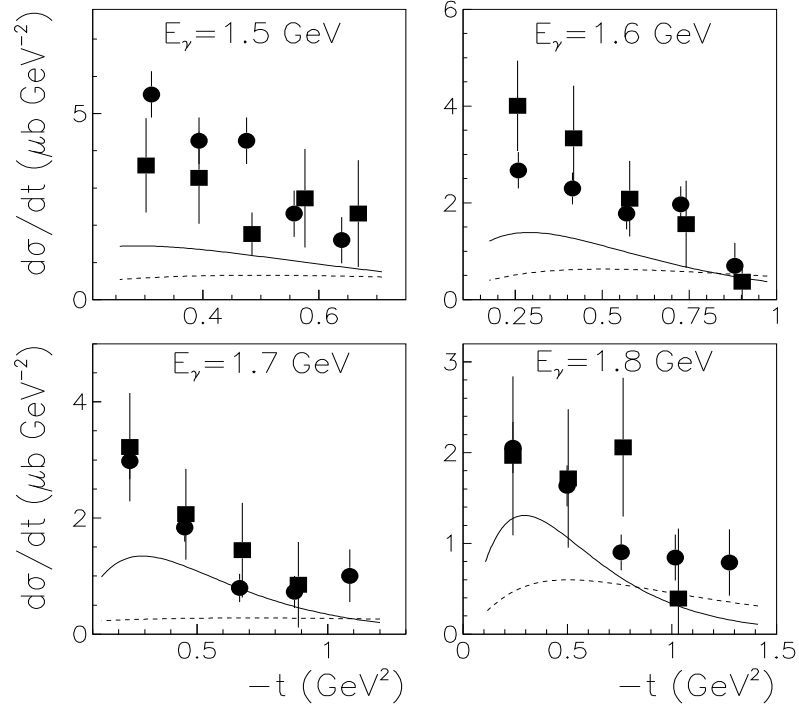


FIG. 3

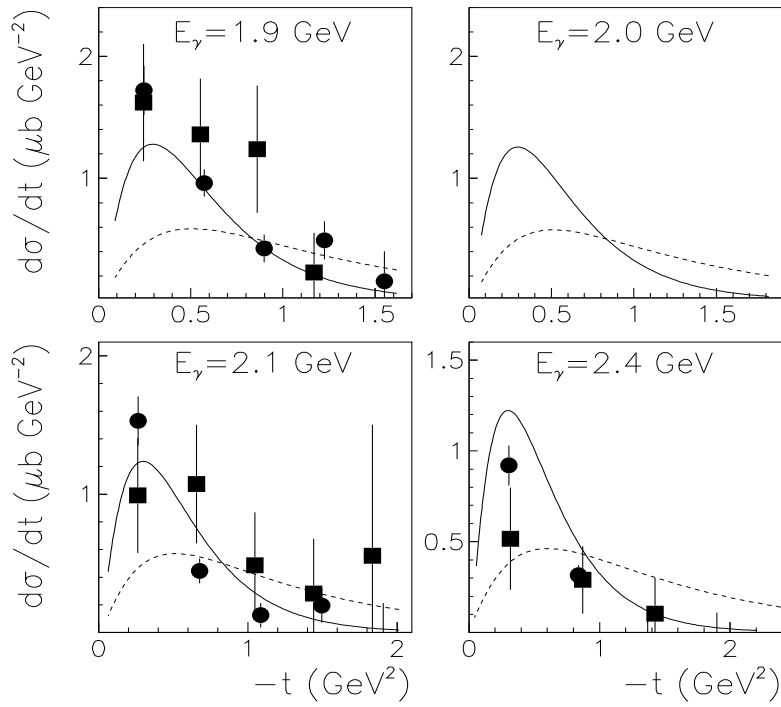


FIG. 4

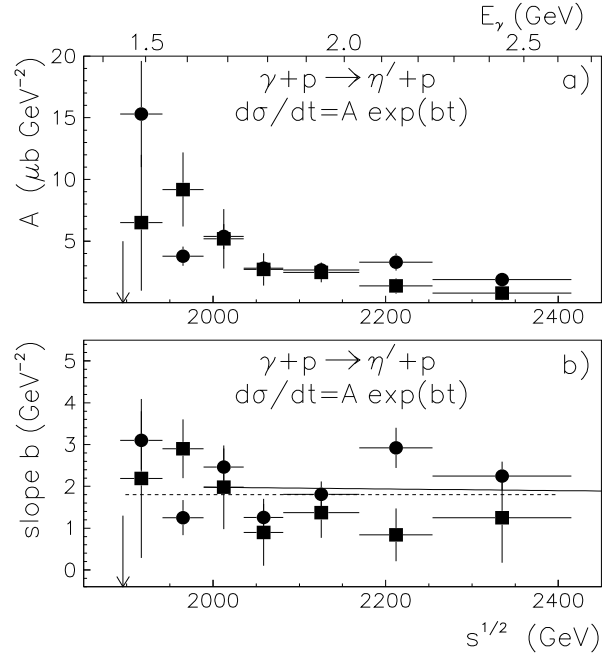


FIG. 5

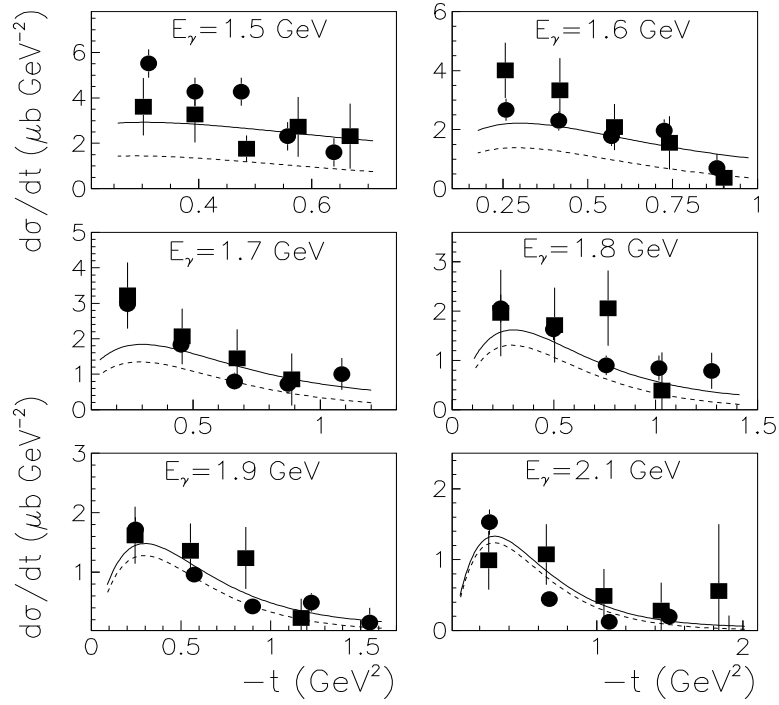


FIG. 6

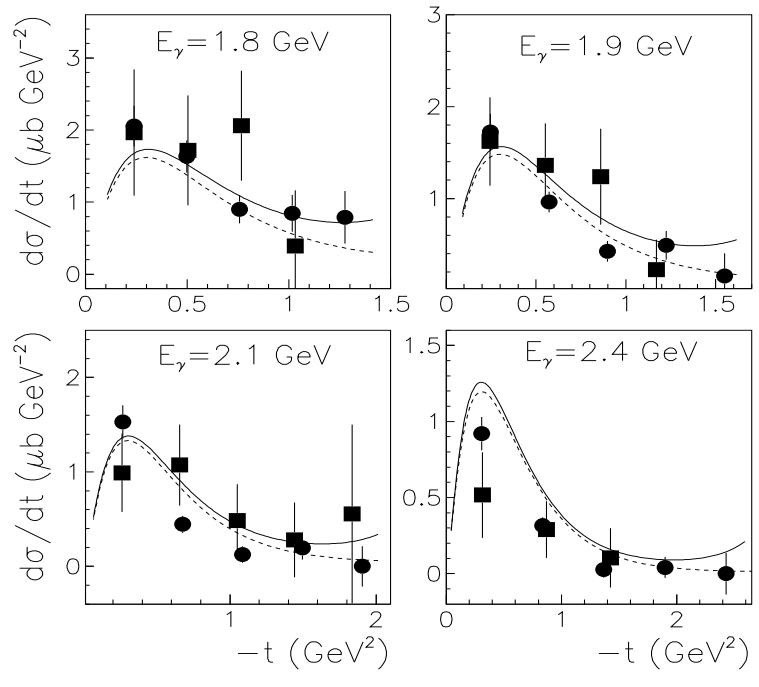


FIG. 7